An Acad Bras Cienc (2022) 94(4): e20211080 DOI 10.1590/0001-3765202220211080
Anais da Academia Brasileira de Ciências | *Annals of the Brazilian Academy of Sciences*
Printed ISSN 0001-3765 I Online ISSN 1678-2690
www.scielo.br/aabc | www.fb.com/aabcjournal

ENGINEERING SCIENCES

Correlating blast vibrations and geomechanical properties to determine damage profiles and improve wall conditions in open pit mining

GUSTAVO S. LOPES, GERMAN VINUEZA, BARBARA TRZASKOS, AUGUSTO F. RIBEIRO & RAFAEL G. ARAUJO

Abstract: Slope stability is one of the biggest concerns for mining practices and to consider the rock mass response over blasting is fundamental to achieve pit geometry. This study consists in developing a methodology which connects the dynamic behavior of one lithological domain to blast designs applied at a copper mine. The central element of this study was the construction of vibration attenuation and seed wave model which, in conjunction with geomechanical properties, has allowed the characterization of this particular rock mass and the vibration attenuation phenomena. The new blast design was developed from the model simulations, once it was possible to recognize which parameters of the blast design affect most of the damage induced by blasting. To guarantee model representativeness, two blast tests were conducted: one with the usual blast design and another using the new one. Furthermore, holes were drilled behind the blasts, which were inspected before and after each blast to compare the produced fracturing with the fracturing expected by the model. The results obtained in these blast tests show a strong correlation between the modeled and the real. The modeling proved to be a useful tool providing manners to stablish a blast design, which generates stable walls.

Key words: Critical PPV, slope stability, induced damage, blasting-induced vibrations.

INTRODUCTION

In the current mining economy, some obstacles to high productivity stand out: the lower value of metals, the high cost of dilution and the expansion of dependence on low-grade mineral deposits. Such facts require the search for an optimized mineral exploitation in which each operation is well controlled, including the control of the damages generated by the rock excavations, subject of the present study.

Among all the factors to be considered while mining, the slopes stability and the fulfillment of the planned pit have significant importance and impact at an efficient and safe mineral exploitation. The increase in the slope angle provides an increase in the strip ratio and consequently the higher cost of mineral extraction. This statement is in accordance with Adamson & Scherpenisse (1998), who state that the development of an open pit mine operations depends, among other factors, on the creation of stable walls.

In order to overcome the obstacles mentioned before, it is extremely important to understand a factor that is usually ignored in the blast design: the rock is heterogeneous, with unique and local characteristics (Singh 2001). Therefore, it is important to consider the geo-mechanical parameters and rock mass structures.

Regarding wall protection, classifications of rock masses such as RMR (Bieniawski 1973), Q (Barton et al. 1974) and GSI (Hoek 1994) are very important, for both geotechnics and rock blasting. In this context, Hoek (2012) introduces the blast damage factor D, which describes the damage caused by the blasting in the rock mass, thus affecting its GSI classification, in particular Bulk Modulus. In addition, it correlates this damage to the bench height, according to parameters used in blast design such as buffer rows and confinement. McKenzie (2016) points out the three main mechanisms of damage caused by blasting: induced vibrations (responsible for creating new fractures), extreme gas pressure (responsible for the expansion of fractures) and release of load (responsible for the creation of fractures parallel to the rock movement). Those are very important factors while addressing pit slope stability.

In this context, many studies have discussed the relationship between blasting, induced vibrations and damage: Ouchterlony et al. (1996), Adamson & Scherpenisse (1998) McKenzie & Holley (2004), McKenzie (2012), Wahyudi et al. (2011) and Onederra et al. (2013). Among these studies, it is important to highlight Adamson & Scherpenisse (1998) and McKenzie (2016), who discussed the effects related to vibration according to Hooke's law and explain the concept of critical peak particle velocity (PPVc), assuming the elastic behavior of the intact rock. According to this concept, PPVc refers to the level of agitation that can be supported by the rock before tensile damage occurs and this value depends on the tensile strength, Young's modulus and primary wave propagation velocity. In these studies, correlations between the vibration peaks and the extent of fracturing are shown. Thus, critical PPV is defined as:

$$PPVc = \frac{\sigma_t \times Vp}{E} \tag{1}$$

Where σ_t is the tensile strength of intact rock (MPa), Vp the primary wave velocity, and E is the Young's modulus.

Furthermore, another very important factor for wall strength preservation is to understand how vibrations and consequently damage are attenuated with distance. Several authors, such as Devine et al. (1966), Blair (1999), Hizen (1998), Silva-Castro (2012), McKenzie (2012), and McKenzie (2013) have studied the behavior of the shock wave generated by the one hole charged with explosive, the seed wave, determining its characteristics (length, velocity, amplitude, frequency) and understanding the relationship between the generation and attenuation of induced vibrations.

This study seeks to assist the staff of an open pit copper mine in Brazil to tackle the challenge of obtaining more stable walls facing blasting induced damage to build a safer and more productive mining operation. The aim is to correlate blasting induced vibrations to damage and build a representative model in order to determine the best blast design to improve wall stability with optimized muck pile´s size distribution. Figure 1 illustrates some slopes of this mine and depicts the challenges of this project: geometry bench issues, such as the loss of crests, the generation of large boulders, and the high degree of damage induced by the actual blasting practice. Figure 1 also shows the slope parameters at this lithological domain.

Although, the actual blast performance regarding muck pile´s size distribution and shape meet the requirements for reasonable plant efficiency. Nevertheless, wall stability and geometry have become an issue due to the high powder factor applied at this domain.

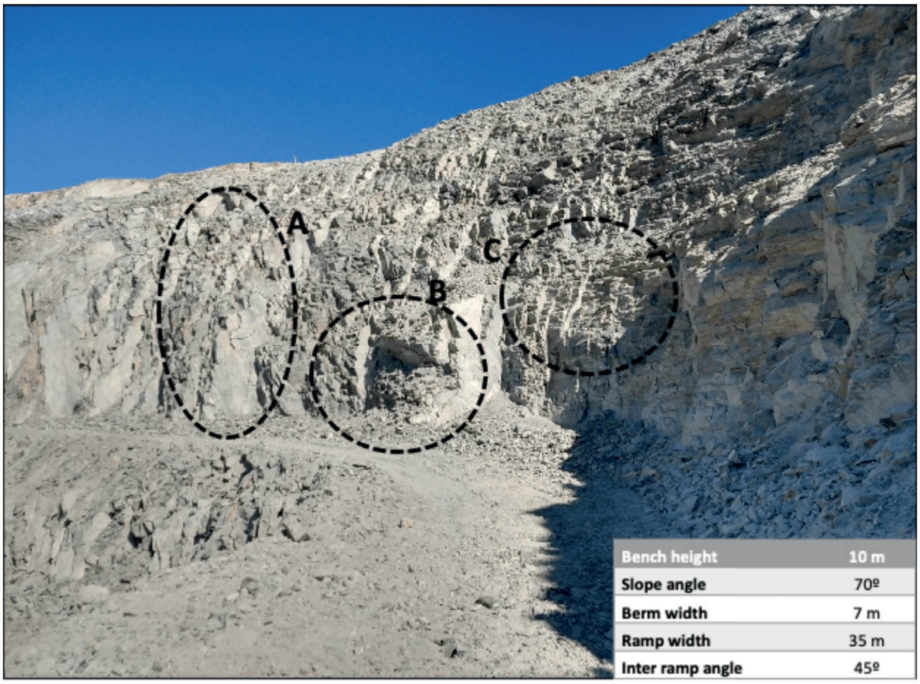

Figure 1. Slope conditions at the mine site and geometrical parameters according to mining staff. A shows geometry issues, B big blocks formed by excessive blast damage and C crest loss.

The biotitite domain was chosen for this study, which according to Miranda et al. (2018) is characterized by the intercalation of biotite schist and amphibole schist, and contains boudinaged amphibolite lenses, muscovite schists containing sericite, as well as hydrothermalized gneiss biotite. This domain was classified into RMR rock mass types II and III. Furthermore, discontinuities sets are well defined, and the influence of hydrothermal alteration can be observed.

METHODOLOGY

This paper discusses the study conducted to generate a vibration attenuation and seed wave model for the biotitite domain of a copper mine used in order to correlate blasting induced vibrations and damage to the rock mass.

As a first step, a cross-hole test, using geophones and small explosive charges, was performed to capture seismic data in near field, characterizing the dynamic interaction between rock mass and the explosive released energy, providing full characterization of waves generated. The geophones'used are shown in figure 2 and their characteristics are described by table I. Mrel's Data Trap II was used to record the information measured with the geophones.

The second step was to generate the equation which characterize the waves' amplitude attenuation due to distance and rock mass heterogeneity. Once wave attenuation was characterized, the second step was to define the limits where vibrations cause damage in this specific rock mass based on the reference values proposed by Adamson & Scherpenisse (1998). These two information enable to correlate Peak Particle Velocity (PPV), damage and distance from the blast and create a model.

This study simulated different blast designs, contemplating two blasts tests to evaluate model effectiveness and it was characterized the damage of these blasts through the inspection of test holes drilled in the close vicinity of the blasts. Figure 3 illustrates the methodology applied in this study.

Figure 2. Geophone used in the field test.

Table I. Geophones technical specifications.

Sensitivity (± 15%)	**290 mV/ips**
Natural Frequency (± 20%)	28 Hz
Coil Resistance (± 5%)	148 ohms
Coil Inductance	45 mh
Damping Factor (± 30%)	0.18
Damping Constant	172
Displacement Limit	0.09 in
Inertial Mass	0.076 oz
Orientation Angle	± 180°
Maximum Velocity	2000 mm/s

Field test and seismic characterization

The first step of this study was to gather the geomechanical parameters that characterize the biotitite. Table II summarizes this information collected from the mine's geology team. Another important information to be considered is the geometric parameters of the expected slope, as shown in Table III, provided by the mine planning team.

Then, a field test was carried out to capture seismic data at near distances, characterizing the dynamic interaction between the rock mass and the detonated explosive charges. Eight holes were drilled, with a diameter of 171 mm and an average depth of 10.4 m, 5m away from each other. The geophones were cemented in the holes G1 and G2, as shown in figure 4. The other holes, Q1-Q6 were charged with bulk emulsion, density 1.15 g/cm^3 and VoD 5400 m/s. All holes were charged with the same explosive charge, 53 kg per hole.

Once the holes were detonated and in possession of vibration information generated in relation to time, it was possible to determine factors such as: propagation velocity P waves (Vp), wave geometric parameters (length, amplitude, period). Figure 5 illustrates the wave form generated by hole Q6 and acquired with geophone 1.

Vibration attenuation and damage model

There are several models and equations from different authors, who sought ways to characterize the phenomenon of attenuation of vibrations with distance. Devine et al. (1966), proposed the model used in this study, due to its easy applicability and representativeness, based on the stepped distance illustrated in equation (2):

$$PPV = K \times \left(\frac{D}{\sqrt{W}}\right)^{-n} \quad (2)$$

Where *PPV* is the peak particle velocity measured in the geophones, *K* is the constant which characterizes the interaction between rock mass and explosive, *W* is the maximum charge blast instantaneously and *n* is the ground attenuation constant. *K* and *n* are determined empirically using a data base containing peak particle velocity and the amount of explosive

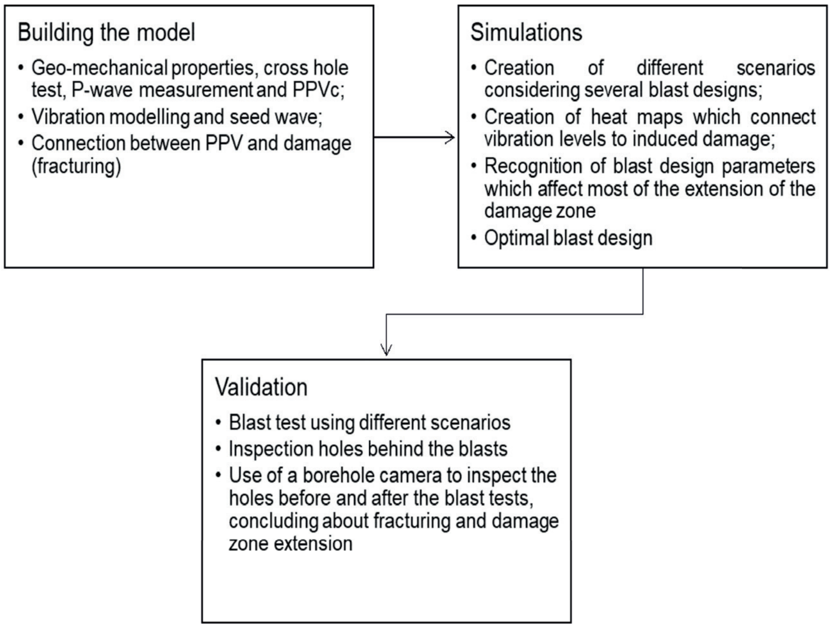

Figure 3. Chart illustrating the methodology steps.

charge which generated it and its respectively distance from the source.

This data allowed the calculation of the vibration attenuation equation in order to characterize this phenomenon. The aim is to define the seismic waves´ parameters and how they attenuate with distance.

This equation was used to calculate de vibration amplitude in different positions upstream the blast. The resultant PPV is gathered from the addition of seed waves (measured in the field test) considering timing and sequencing and scaling charge and distance, using equation 2, as proposed by Blair (1999), generating the vibration attenuation and seed wave model.

Correlation between vibration and damage

According to Adamson & Scherpenisse (1998), there is a close relationship between fracturing and PPV and it is described as shown in Table IV. Therefore, once vibration attenuation phenomenon was characterized, the next step was to define which vibration thresholds cause damage at the rock mass, the critical PPV.

The geomechanical properties of the rock mass gathered with geology mining team and the P-wave velocity acquired during the field tests enabled to calculate the critical PPV.

The author connected the vibration attenuation model and the expected vibration levels with the effect (damage) as a function of the critical PPV. This combination allowed creating a model which generated vibration heat maps to analyze the damage extension behind the blasts, according to each blast design tested.

Table II. **Biotitite geomechanical properties.**

UCS (Mpa)	118
E (Gpa)	54
Poisson	0.37

Table III. **Actual designed slope parameters.**

Bench Height	10 m
Bench Angle	70º
Berm width	7 m
Ramp width	35 m
Inter-ramp angle	45º

Figure 4. Test configuration where G1 and G2 are the two geophones installed and Q1-12 are the holes with explosive charges.

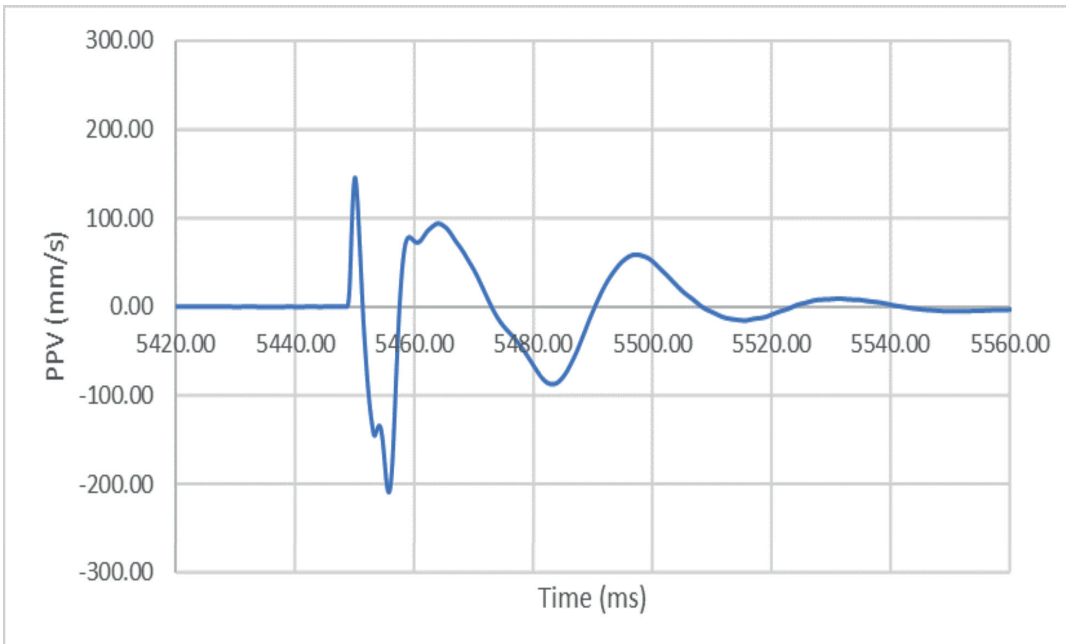

Figure 5. Waveform recorded at G1 from hole Q6 – Longitduinal Axis.

Simulations

The next step was to conduct simulations to understand damage propagation and define the blast design to be utilized in the blast tests. In accordance with operational restrictions, such as borehole diameter, explosives and bench height, different simulation scenarios were defined as described by table V.

Scenarios H and I take into account buffer lines which were dimensioned to reduce blast induced vibration on the slope and, consequently, reduce the damage. Table VI describes the buffer's design.

Vibration heat maps were generated for each scenario where the expected induced vibration was analyzed and compared with the PPV_c of the studied lithological domain. These heat maps permitted to determine which blast design would provide a better slope condition (reducing the damage), thus permitting to define, within the mine operational restrictions, which drilling and blasting configuration should be selected for testing to compare with the currently adopted at the mine site (A).

Table IV. Relationship between damage and PPV.

PPVc ratio	Effects
1/4 PPVc	Fracture dilatation
PPVc	New fractures appearance
4xPPVc	Intense fracturing
8xPPVc	Rock pulverization

Table V. Blast designs simulated using the model.

	Diameter (mm)	Burden (m)	Spacing (m)	Bench Height (m)	Sequencing (regarding the slope)	N Rows	Buffer Rows.
A	171	4	4.5	10	Paralel	8	n
B	171	4	4.5	10	Paralel	10	n
C	171	4	4.5	10	Paralel	12	n
D	171	4	4.5	10	Perpendicular	8	n
E	171	4.8	5.5	10	Paralel	8	n
F	251	4.8	5.5	10	Paralel	8	n
G	171	4	4.5	20	Paralel	8	n
H	171	4	4.5	10	Perpendicular	8	1
I	171	4	4.5	10	Perpendicular	8	2

Table VI. Buffer design details.

Burden (m)	4
Spacing (m)	2.1
Hole diammeter (mm)	171
Hole length (m)	10
Stemming (m)	3
Air Deck (m)	3
Charge Length(m)	3.5

Blast tests

Two blast tests were conducted nearby in order to evaluate the simulations's findings. One of the test adopted the scenario A and the second adopted scenario H. They were executed at the same domain of the field test aiming to have similar conditions.

A borehole camera was used to inspect the drillholes specially made upstream of the two blast tests in order to confirm the damage indications of the vibration heat maps, and the effectiveness of the proposed blast design in reducing blasting damage. These images were used to identify the degree of fracturing of the rock mass and counting it before and after the blasts, which allowed correlating the modeled levels of vibration with the fracturing increase, therefore permitting to validate the proposed model.

RESULTS

The gathered data in the cross-hole testing enabled to obtain an average value of *Vp* (primary wave propagation velocity) of 4926 m/s. This value, which is considerably high, indicates high competence of the rock mass, corroborated by its geo-mechanical information, gathered from the mine staff: UCS of 118 MPa and Young Modulus of 51 GPa. Thus, using Equation 1, it was possible to determine the critical PPV characteristic of this rock mass. The value found for biotitite in site conditions was 1139 mm/s.

The data obtained in the field was sufficient to generate a vibration attenuation model of high correlation. Equation 2 highlights the applicable equation, according to the reference work of Devine et al. (1966). Thus, the K value found is 725 and the n value is -1.81, with a correlation coefficient (R^2) of 0.92.

$$PPV = 725 \times \left(\frac{D}{\sqrt{W}}\right)^{-1{,}81} \tag{2}$$

In view of the expected damage as a result of PPVc, heat maps that correlate vibration and damage were generated for each of the considered scenarios. The results of each scenario were compared with scenario A (commonly used in the mine) to determine, within the blast design parameters range, those that contribute most to the rock mass blast-induced damage.

Table VII presents the relationship between damage extension and bench height, as proposed by Hoek (2012). The damage extension was measured from the slope until the border of the zone where the PPV level was smaller than a quarter of PPVc. It is very important to consider this damage extension as the change of the rock bulk modulus and consider the impacts of this change at the rock mass quality and its effect at slope stability.

These findings were the fundamentals for the definition of an optimized but feasible blast design considering the existent drilling equipment, however being safer and delivering higher productivity.

The damage extension of each scenario was calculated based on the damage model being compared with the bench height, as suggested by Hoek (2012). The values found are in accordance with Hoek´s statements, varying only for scenario G, with a bench height of 20 m and, according to the model, corresponding just to a 23% damage increase in comparison to the base scenario A. Thus, the ratio of bench height and damage extension is 1.1, the smallest value simulated. The results in Table II show that adequate timing and sequencing and the use of buffer rows promote a strong impact on damage, corroborating the results stated by McKenzie (2016).

According to the modeling results, scenarios A and H were chosen to be tested in the mine: A is the one that is already in use, while H was chosen due to the considerable reduction of expected damage in contrast with the relatively minimal efforts for its application (since the use of more than one buffer rows would considerably increase the number of drilled holes).

The Figure 6 shows the area of both tests. It illustrates the location of the blasts and the main geological structures of the area. It brings to attention the proximity of both blasts and its similar conditions, presenting the same predominant rock mass and main structures.

Figure 7 illustrates the first blast test, with the blast design referring to scenario H, and its respective heat map, showing the location

Table VII. Comparison between the expected damage extensions for the different scenarios.

Scenarios	Damage Extension (m)	Variation	Bench height ratio
A	17.7	-	1.8
B	17.9	+1%	1.8
C	17.4	-1%	1.7
D	16.5	-7%	1.6
E	16.6	-6%	1.7
F	20.0	+13%	2.0
G	21.7	+23%	1.1
H	13.1	-26%	1.3
I	10.1	-43%	1.0

of the inspection holes (holes upstream of the polygon) and in black the slope after the blast, indicating a good geometrical adherence between modeling and reality. The inspected holes are 2m away from each other and the first inspected hole was drilled 7m away from the last row of boreholes.

Figure 8 shows images captured while inspecting the holes. The inspection of the other two holes suggests a significant reduction in the damage level, illustrated by figure 8b and c.

These results corroborate the indications of the damage model, which suggest the more intense appearance of fractures in the first inspection hole and considerable reduction in the second and third holes. Thus, according to these findings the real damage extension is around 12-13 m due to the reduction of fracturing in the last hole inspected. Table VIII shows the details of the fracturing intensity pre and post blast test 1.

The same procedure was repeated in the second blast test using the design described for scenario A and due to operational limitations just two holes were drilled for inspection. Figure 9 shows the heat map of this blast test, highlighting the remaining slope in black, showing a large discrepancy between the planned and the executed.

This time, due to the non-use of buffer rows and appropriated timing and sequencing, very extensive damage was observed causing the collapse of the first hole inspected and very intense fracturing at the second one. Figure 10 shows images of the holes inspected, with a high degree of damage and the collapsed hole (5C). Table IX shows the details of the fracturing intensity pre and post blast test 2.

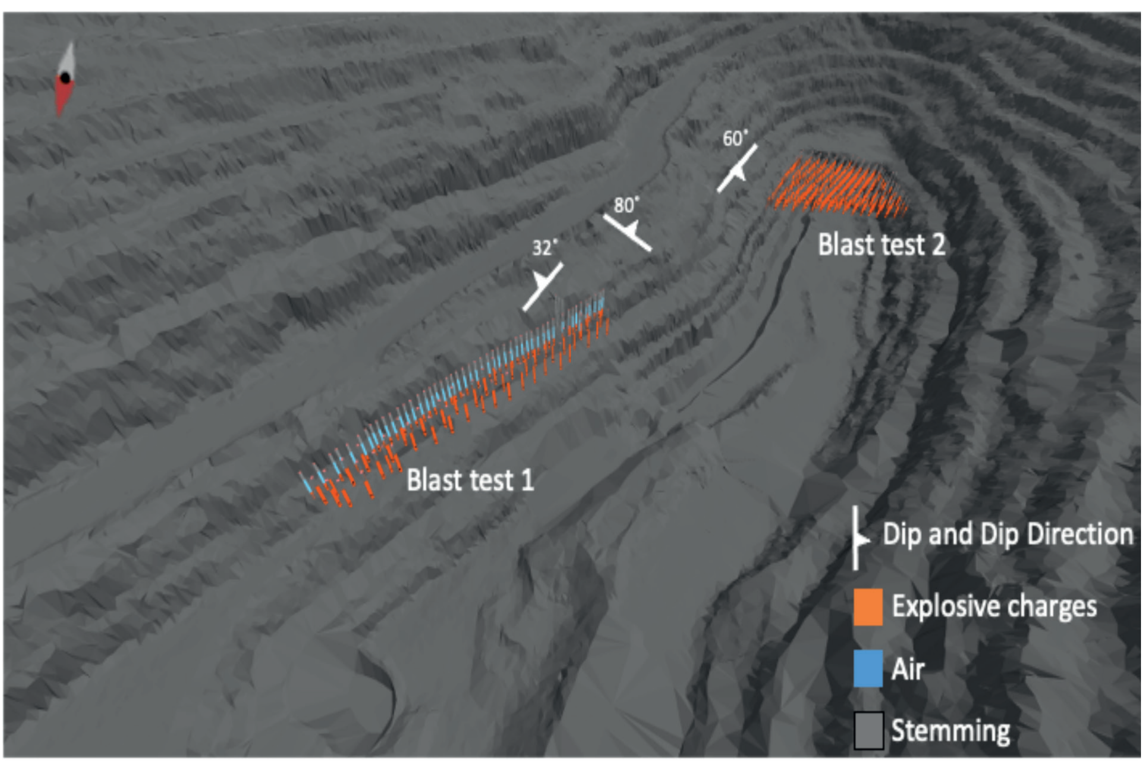

Figure 6. **Area of the blast tests and their direction and dip direction of the region's main discontinuity sets.**

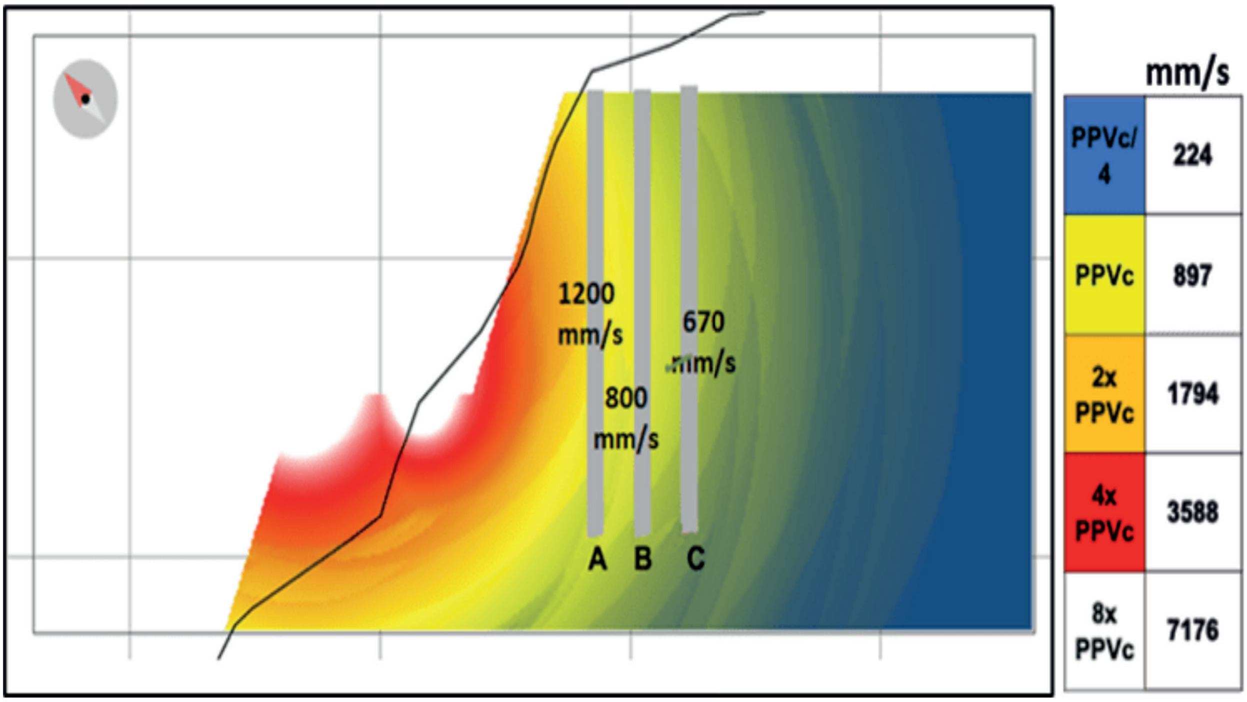

Figure 7. Vibration heat map showing the inspected holes A B C in gray, expected induced damage based on PPVc and the actual slope in black for blast test 1. Fracturing is expected throughout the yellow zone and the distance between the last row of boreholes until its border is around 13 m.

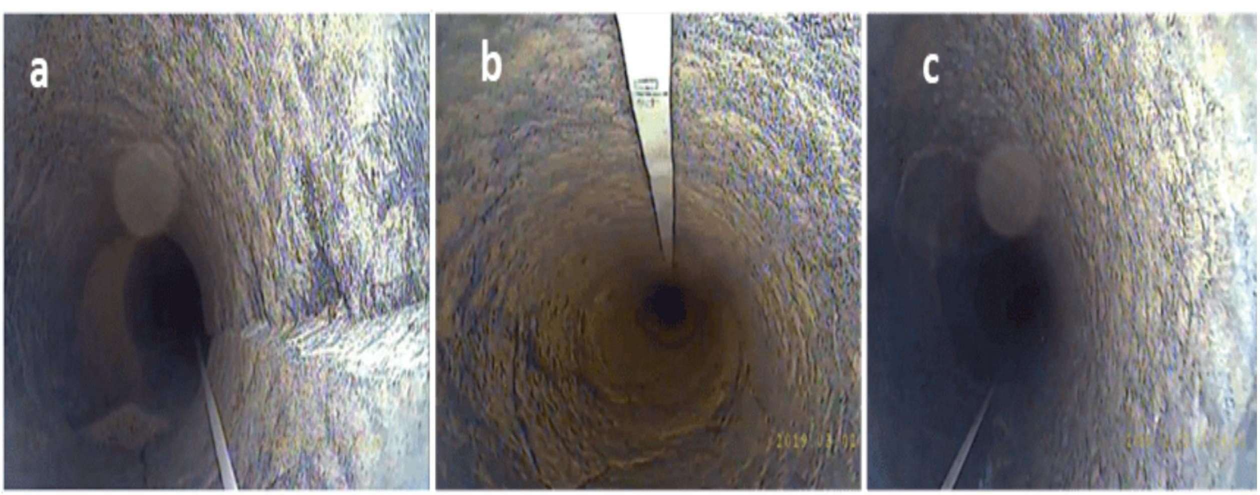

Figure 8. Images from the inspected holes of blast test 1. A has been made in the upper third of hole a, while b and c show the reduction of fracturing of holes b and c, both represented in Figure 3.

Table VIII. Fracturing intensity pre and post blast test 1.

	Distance from the last row (m)	N fractures pre blast	N fractures post blast	Difference
Hole a	6.10	11	30	173%
Hole b	7.97	11	13	18%
Hole c	9.81	6	6	0%

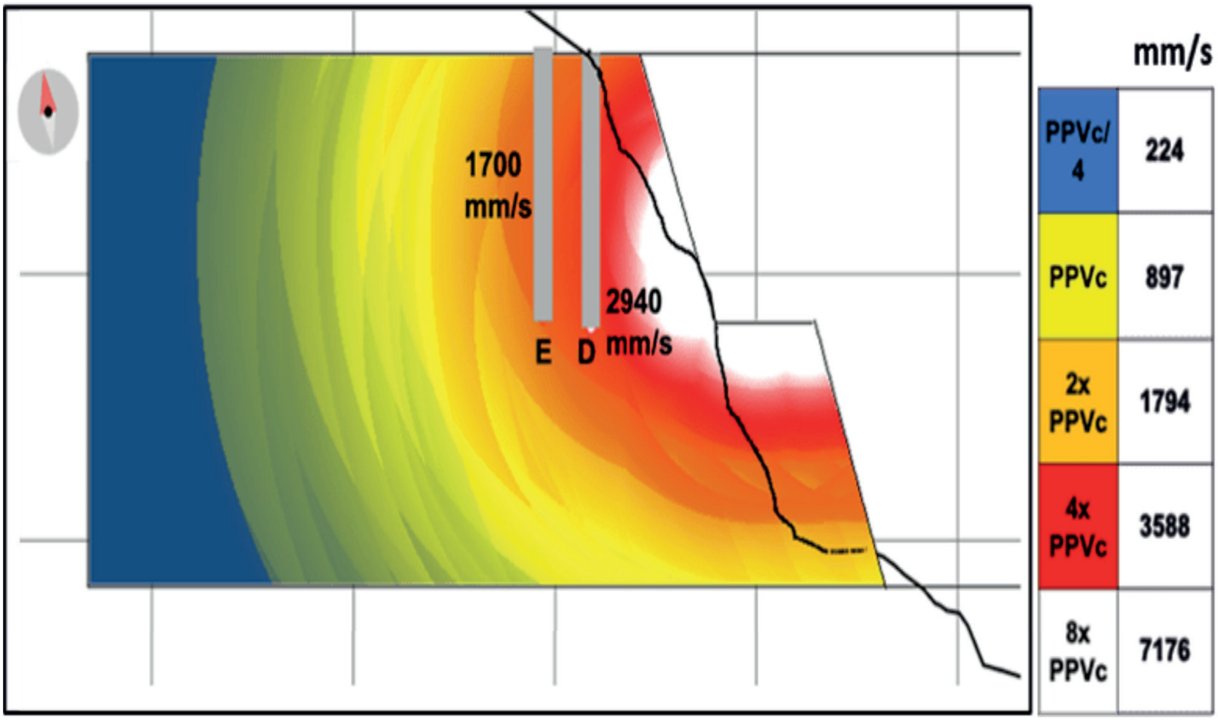

Figure 9. Vibration heat map showing the inspected holes in gray, expected induced damage based on PPVc and the actual slope in black for blast test 2. Fracturing is expected throughout the yellow zone and the distance between the last row of boreholes until its border is around 21

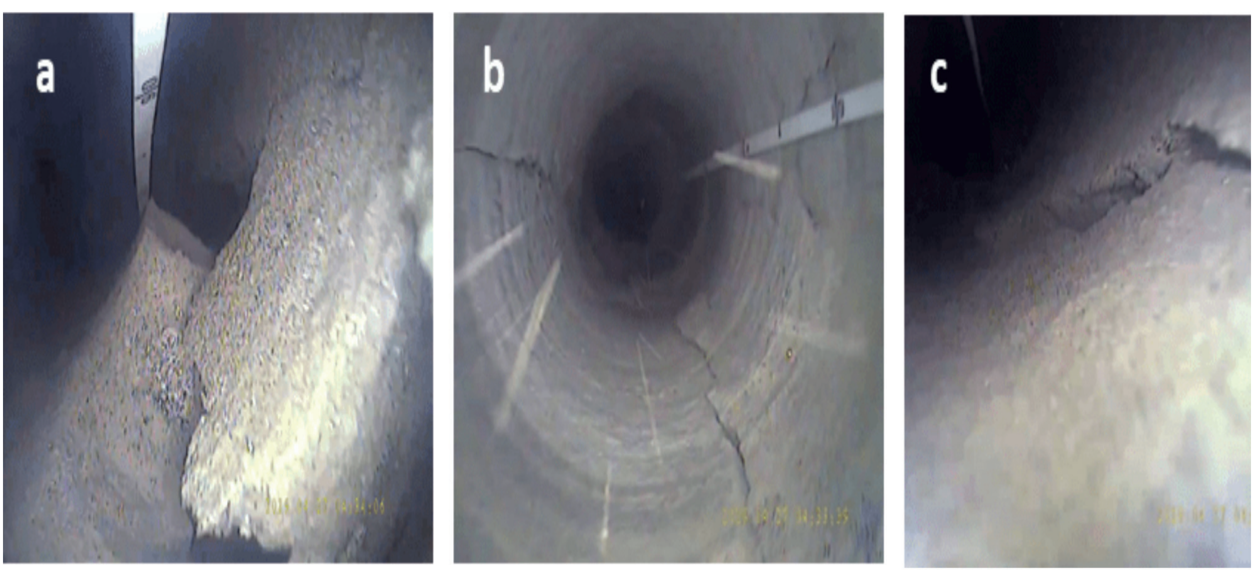

Figure 10. Images from the inspection holes of blast test 2. a has been made in the collapsed hole d, while b and c show the intense fracturing of hole e, both represented in Figure 5.

Table IX. Fracturing intensity pre and post blast test 2.

	Distance from the last row	N fractures pre blast	N fractures post blast	Difference
Hole d*	5.3	4	4	0%
Hole e	7.4	7	15	114%

*** Hole d was collapsed and it was impossible to determine the increase of the number of fractures properly.**

DISCUSSION

The first blast test, where an appropriate buffer row, timing and sequencing were used, only the first third of the inspected holes did not fulfilled the modeling prediction, since it was observed a strong disturbance of the hole shape. It is believed that this fact is a side effect of excessive subdrilling used in the blast of the upper bench, which it has caused a significant damage at the top part of the blast test one. Thus, this is supported by the high vibration profile observed at the berms in the heat maps.

In the second blast test, with no buffer rows and where the direction of the blast was parallel to the slope, strong adherence between modeling and reality was observed, since high vibration levels were expected in the first inspection hole. The collapse of the closest inspected hole highlights this fact and strengthens the representativeness of the damage modeling indications.

The results observed in field for these two blasts tests showed a strong correlation with the modeling results, as registered in the images obtained with the borehole camera. This fact proves that this methodology is a useful tool for building a blast design to reduce wall damage. Thus, the results of simulations and the blast test has shown the importance of the use of buffer rows and appropriated timing and sequencing, since it was observed significant reduction in the number of fracturing and respectively damage where this technique was applied.

Furthermore, the reduction of the vibration levels by using buffer rows and appropriated timing reduced the impact of blasting at the rock mass, not affecting the bulk modulus as much as blasting without any control. Due to this fact, the use of this technique helped to improve slope stability as the damage zone extension is smaller. The model helped to identify the changes of damage zones according to the blast design providing guidance to address the challenge of more stable walls. Although the number of fractures pre and post blast were surveyed, it was not possible to estimate RQD due to equipment limitations (the borehole camera did not have meter count).

CONCLUSION

This study has presented a feasible methodology to achieve more stable walls taking into account site particularities. The results were in accordance with the studies presented in the introduction section. The Blast Damage Factor is a great guide to geotechnical teams at mines, which can improve their modeling using this methodology to consider site-specific assessments.

The results obtained in the simulations and blast tests showed a strong correlation between the modeling results and the field observations, validating the values presented in Table II.

This methodology can help to implement new practices to promote wall control blasting and consequently more stable slopes. This is because the model can be used to analyze the extension and level of damage zones (consequently rock bulk modulus degradation) created behind the blasts and the influence of each blast design parameters.

Furthermore, the key factors which influences most fracturing and consequently damage at pit walls were presented in respect of the studied domain. Upon the review of literature and as stated by authors, it has been proven significant influence of blast design factors, such as sequencing and buffer rows, at the PPV levels and consequently induced damage.

As a further work, it is proposed to conduct more blast tests in order to increase the data set to confirm the findings and also install a meter count in the camera to estimate RQD. Furthermore, the same methodology should be replicated to other domains in this mine site and other mine sites to support the findings presented here.

Acknowledgments

Many thanks to the entire Graduate Program in Geology at the Federal University of Paraná for offering all the means for the development of knowledge in geosciences and the realization of this study. I would also like to thank all my colleagues at Enaex, especially those at EMTS, for all the support and dedication in carrying out the work that was developed here. This research did not receive any specific grant from funding agencies in the public, commercial, or not-for-profit sectors.

REFERENCES

ADAMSON WR & SCHERPENISSE CR. 1998. The measurement and control of blast induced damage of final pit walls in open pit mining. International Society of Explosive Engineers, p. 1-16.

BARTON NR, LIEN R & LUNDE J. 1974. Engineering classification of rock masses for the design of tunnel support. Rock Mech 6(4): 189-239.

BIENIAWSKI ZT. 1973. Engineering Classification of Jointed Rock Masses. Trans S Afr Inst Civ Eng 15: 335-344.

BLAIR DP. 1999. Statistical Models for Ground Vibrations and Airblast. International Journal of Blasting and Fragmentation. Rotherdam, Netherlands, p. 335-364.

DEVINE JF, BECK RH & MEYER AVC & DUVALL WI. 1966. Effect of Charge Weight on Vibration Levels from Quarry. United States Department of The Interior. Washington USA, p. 1-41.

HIZEN KG. 1998. Modeling of Blast Vibration. Int J Rock Mech Scl. & Geomech Abstr 25(6): 439-445.

HOEK E. 1994. Strength of Rock and Rock Masses. News Journal of ISRM 2(2): 4-16.

HOEK E . 2012. Blast Damage Factor, D, Technical note for Rocscience, p. 1-8.

MCKENZIE CK. 2012. Limits Blast Design: Controlling Vibration, Gas Pressure & Fragmentation, Proc. 10th International Symposium on Rock Fragmentation by Blast, Fragblast 10 (Eds: Singh & Sinha), New Delhi, India, p. 1-10.

MCKENZIE CK. 2013. Seed Wave Modelling Applications for Fragmentation, Damage, and Environmental Impact Control. Blasting in mines – New Trends, p. 1-14.

MCKENZIE CK. 2016. Blasting near open pit walls, Proceedings of the First Asia Pacific Slope Stability in Mining Conference, Australian Centre for Geomechanics, Perth, p. 83-94.

MCKENZIE CK & HOLLEY K. 2004. A study of damage profiles behind blasts, Proc. 30th Annual Conference on Explosives and Blasting Technique, International Society of Explosives Engineers, New Orleans, LA 2: 1-13.

MIRANDA HM, MOORE CM, PATEL A & PIGNATARI LEC. 2018. Technical Report on The Chapada, Mine Goiás State, Brazil. NI 43-101 Report, Toronto, p. 7-14.

ONEDERRA I, CATALAN A & CHITOMBO G. 2013. Modelling fracturing, disturbed and interaction zones around fully confined detonating charges. Institute of Materials, Minerals and Mining and The AusIMM, Mining Technology 122: 20-32.

OUCHTERLONY F, NIE S, NYBERG U & DENG J. 1996. Monitoring of large open cut rounds by VOD, PPV and gas pressure measurements, Proc. 5th International Symposium on Rock Fragmentation by Blasting - Fragblast 5 (Ed: B Mohanty), p. 3-26.

SILVA-CASTRO JJ. 2012. Blast Vibration Modeling Using Improved Signature Hole Technique for Bench Blast. College of Engineering at the University of Kentucky. Lexington, USA, p. 1-236.

SINGH SP. 2001. The influence of geology on blast damage. Sudbury, Laurentian University, p. 121-127.

WAHYUDI S, SHIMADA H, SASAOKA T, KUBOTA S, OGATA Y & MATSUI K. 2011. Prediction of Near-Field Rock Damage Due to Production Blasting in Limestone Quarries. Mine planning and equipment selection (mpes) conference, Fremantle, p. 1-13.

How to cite
LOPES GS, VINUEZA G, TRZASKOS B, RIBEIRO AF & ARAUJO RG. 2022. Correlating blast vibrations and geomechanical properties to determine damage profiles and improve wall conditions in open pit mining. An Acad Bras Cienc 94: e20211080. DOI 10.1590/0001-3765202220211080.

Manuscript received on August 1, 2021;
accepted for publication on December 1, 2021

GUSTAVO S. LOPES[1]
https://orcid.org/0000-0002-9369-8756

GERMAN VINUEZA[1]
https://orcid.org/0000-0001-8341-3107

BARBARA TRZASKOS[1]
https://orcid.org/0000-0002-3000-3531

AUGUSTO F. RIBEIRO[2]
https://orcid.org/0000-0001-8024-3966

RAFAEL G. ARAUJO[3]
https://orcid.org/0000-0002-7894-7531

[1]Universidade Federal do Paraná/UFPR, Departamento de Geologia Av. Cel. Francisco H. dos Santos, 100, Jardim das Américas, 81530-000 Curitiba, PR, Brazil

[2]Enaex Britanite, EMTS, Rod. Régis Bittencourt, s/n, Jardim Pinheiros, 83420-000 Quatro Barras, PR, Brazil

[3]Yamana Gold, Departamento de Perfuração e Desmonte, Rua Natal, 106-174, 76560-000 Alto Horizonte, GO, Brazil

Author contributions

Conceptualization, GSL, GV, BT and RGA.; methodology, GSL, GV and BT.; field work, GSL, AFR and RGA formal analysis, GSL, GV, BT, RGA and AFR.; resources, GSL, AFR e RGA.; data curation, GSL.; writing—original draft preparation, GSL, GV and BT.; writing—review and editing, GSL, GV and BT; discussion, GSL, GV, BT, AFR and RGA. All authors have read and agreed to the published version of the manuscript.